EPJ Web of Conferences **114**, 02116 (2016)
DOI: 10.1051/epjconf/201611402116

An experimental investigation of flow around a vehicle passing through a tornado

Masahiro Suzuki[1,a], Kouhei Obara[1] and Nobuyuki Okura[1]

[1]*Meijo University, Department of Vehicle and Mechanical Engineering, 468-8502 Nagoya, Japan*

Abstract. Flow around a vehicle running through a tornado was investigated experimentally. A tornado simulator was developed to generate a tornado-like swirl flow. PIV study confirmed that the simulator generates two-celled vortices which are observed in the natural tornadoes. A moving test rig was developed to run a 1/40 scaled train-shaped model vehicle under the tornado simulator. The car contained pressure sensors, a data logger with an AD converter to measure unsteady surface pressures during its run through the swirling flow. Aerodynamic forces acting on the vehicle were estimated from the pressure data. The results show that the aerodynamic forces change its magnitude and direction depending on the position of the car in the swirling flow. The asymmetry of the forces about the vortex centre suggests the vehicle itself may deform the flow field.

1 Introduction

The tornado is a violent meteorological phenomenon. It sometimes damages infrastructures severely. It rarely hits moving ground vehicles. However, once it occurs it would bring a huge damage. Actually, several train-over-turned accidents with casualties by tornadoes have been reported in Japan [1, 2].

The tornado has been studied by means of field observation, analytical approach and computational simulation in terms of meteorology and civil engineering. Meteorologists have tried to clarify the structure of the tornado and its mechanism, while civil engineers have managed to reduce the damage of the infrastructure. Recently, Hann et al. have developed a tornado simulator. It generates tornado-like vortices to quantify aerodynamic forces on civil engineering structures [3].

The crosswind stability of the ground vehicles has been vigorously studied in the past. Those works mainly concern steady/unsteady winds coming from one direction. The tornado like swirling flow has been barely investigated in spite of its risk to our society.

Therefore we have been investigated the effect of the tornado on the moving ground vehicle. In this paper, we describe our experimental approach by use of a tornado simulator based on Hann's study.

2 Method

Our experimental setup was composed of the tornado simulator and a moving model rig. Figure 1 shows the setup. The tornado simulator had a fan, an inner and an outer duct, 18 guide vanes and a stage (Fig. 2). The fan produced an upward flow in the inner duct. Then the flow passed between the guide vanes. The guide vanes that were attached at an angle created a twisted downward flow in the outer duct and a tornado-like swirling flow on the stage. The swirl ratio, S, is an

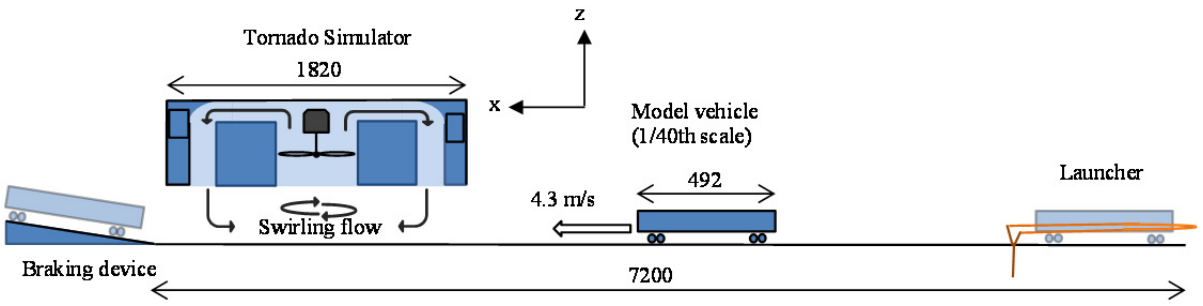

Figure 1. Experimental setup (unit: mm).

[a] Corresponding author: msuzuki@meijo-u.ac.jp

important parameter and has a close relation with the flow structure of the tornado. It is the ratio of the angular momentum to the updraft momentum and is defined as follows:

$$S = \frac{r}{2H}\tan\theta \quad (1)$$

Here, r is the radius of the inner duct, H is the height of the convergence layer (see Fig. 2(b)) and θ is the guide vane angle. In our experiment, the swirl ratio can be adjusted by changing the guide vane angle. The guide vane angle was set at 30°, 40°, 50° and 60°.

The moving model rig had a straight track, a model vehicle, a launcher and a breaking device. The track was placed in such a way the vehicle passed through the center of the vortex. The model vehicle had a train-like shape with a scale of 1/40 (Fig. 3). The vehicle had 72 pressure ports on its surface. Pressure sensors and data logger with AD converter were loaded inside the vehicle. The launcher accelerated the vehicle to 4.3 m/s by using an elastic force provided by rubber bands. A motor inside the vehicle rotated wheels to keep the speed constant. The braking device stopped the vehicle softly and safely.

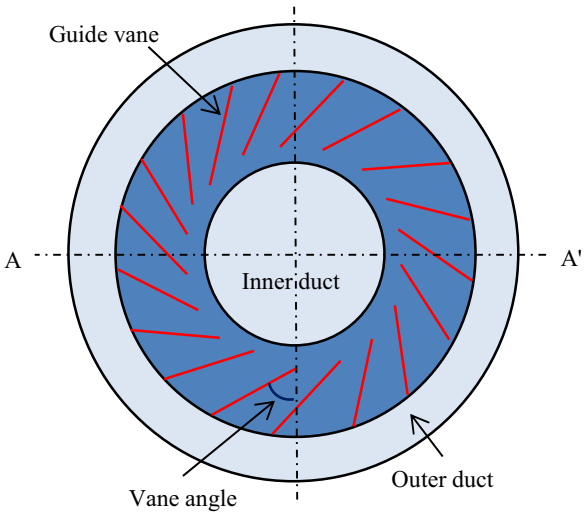

(a) Top view.

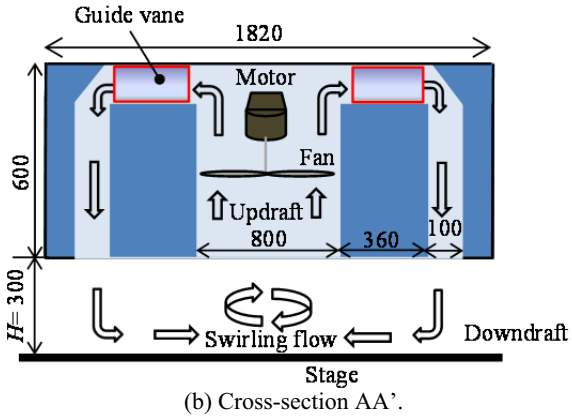

(b) Cross-section AA'.

Figure 2. Tornado simulator (unit: mm).

The flow field generated by the tornado simulator was measured by PIV. Note there were no vehicles in this measurement. The cross-sectional velocity distributions on the horizontal plane at z = 0.54R (the centre height of the vehicle body) and the vertical planes at the centre of the swirling flow were examined. The pressure distribution on the stage was also measured.

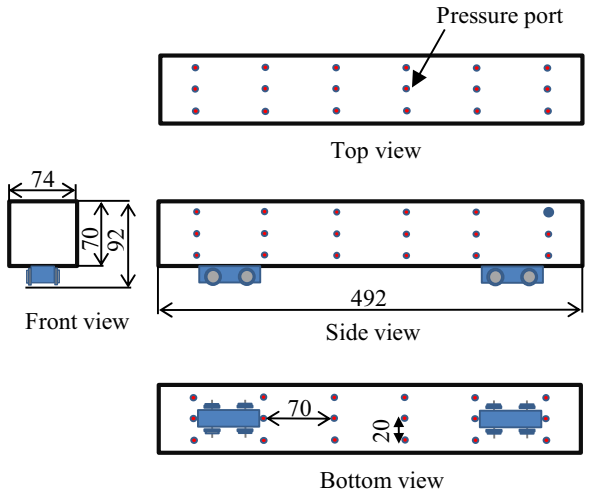

Figure 3. Model vehicle (unit: mm).

3 Results

3.1 Flow field generated by the tornado simulator

Figure 4 shows an example of the velocity vectors obtained by the PIV measurement. The swirl ratio, S, is 0.79 in this case. Colours of the vectors indicate the magnitude of the velocity on each plane. The velocity vectors on the horizontal plane clearly show the swirling flow field. The velocity vectors on the vertical plane indicate that the flow coming from the far field near the stage moves up while a weak downdraft appears in the centre area. This is flow structure is called a two-celled vortex [3]. By using the velocity field obtained by PIV, the maximum tangential velocity, *Vmax*, and the radius of vortex core, *R*, at which the tangential velocity becomes maximum were obtained in each case of the vane angle (Table 1). As the Swirl ratio increases, the radius of vortex core increases. The tangential velocity also becomes larger at $\theta < 60°$.

Figure 5 shows normalized tangential velocity profiles at the horizontal plane. The horizontal axis indicates normalized distance from the vortex centre. Doppler radar data from full-scale tornados at Spencer, South Dakota and Mulhall, Oklahoma [3] are also plotted in the figure. The height of the horizontal plane of these full-scale tornado data is $z = 0.52R$, while ours is $z = 0.54R$. A black thin line displays the theoretical value of the Rankin vortex model, which a widely-used simple model of the tornado [4]. The model defines that a tangential velocity in the inner region is proportional to

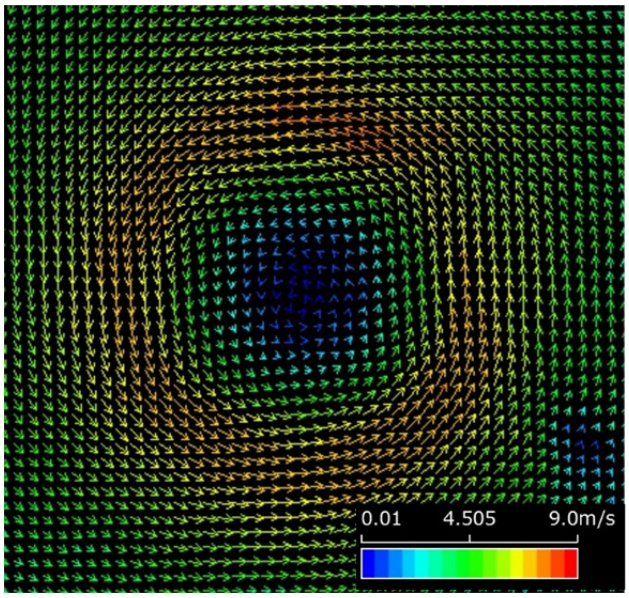

(a) Velocity vectors on the horizontal plane ($z = 0.54R$).

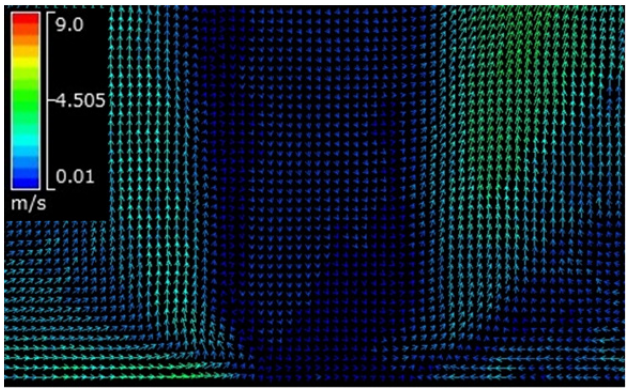

(b) Velocity vectors on the vertical plane at the vortex centre.

Figure 4. Velocity vectors of the vortex.

Table 1. Maximum tangential velocity and radius of vortex core.

θ (degree)	S	*Vmax* (m/s)	*R* (mm)
30	0.38	6.1	74
40	0.56	6.8	89
50	0.79	7.4	96
60	1.15	7.0	115

the distance from the centre, x, while it is inversely proportional to the distance in the outer region as follows:

$$V(x) = \begin{cases} V_{max}\frac{|x|}{R} & , \ |x| \le R \\ V_{max}\frac{R}{|x|} & , \ |x| > R \end{cases} \quad (2)$$

While our results disagree with the Rankin vortex mode at *r/ R* >1, they agree well with the radar data irrespective of the vane angle.

Figure 6 illustrates the pressure distribution on the stage in the case of $\theta = 50°$. A line indicates the Rankin vortex model. Pressure distribution of the Rankin vortex model is as follows:

$$p(x) = \begin{cases} \frac{1}{2}p_{min}\left[2 - \frac{x^2}{R^2}\right] & , \ |x| \le R \\ \frac{1}{2}p_{min}\frac{R^2}{x^2} & , \ |x| > R \end{cases} \quad (3)$$

Here, p_{min} is the minimum value of the pressure. Our experimental result agrees well with the Rankin vortex model except near the vortex centre. Hann et al. also observed this flattened profile near the vortex centre [3]. They suggested that this is due to the downdraft near the vortex centre that was also observed in our PIV measurement.

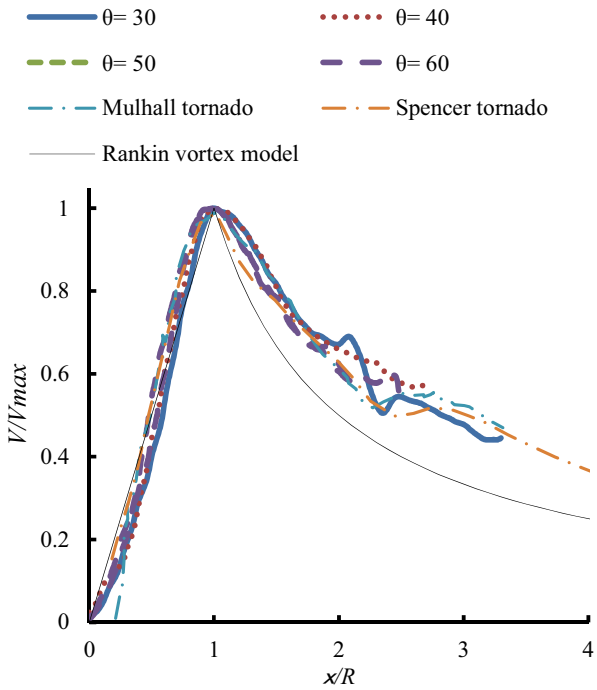

Figure 5. Tangential velocity profiles.

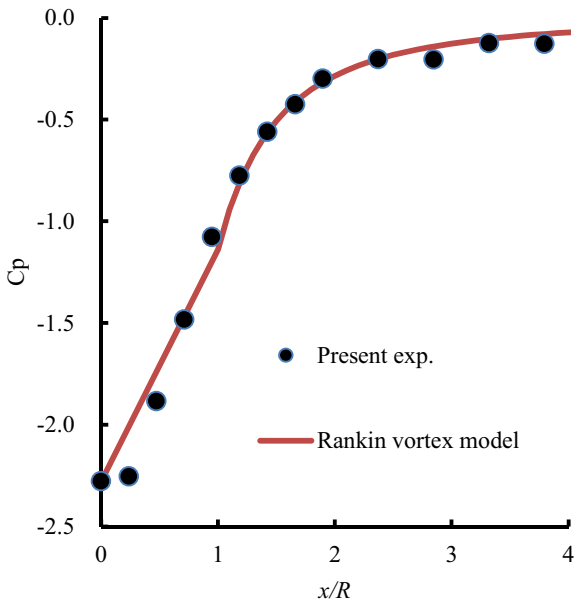

Figure 6. Pressure distribution on the stage ($\theta = 50$).

3.2 Aerodynamic forces acting on the moving vehicle

When the measurement of surface pressure on the vehicle running in the tornado was conducted, the vane angle of the tornado simulator was set at 50 degrees. The corresponding Reynolds number based on the maximum tangential velocity and the vehicle length was 2.2 x 10^5.

The aerodynamic forces were obtained by using the ensemble averaged surface pressure data of 30 runs. Figure 7 explains the definition of the aerodynamic forces and moment acting on the vehicle. Figure 8 presents time histories of the side coefficient, Cs, the lift force coefficient, Cl, and the yawing moment coefficient, Cy, of the moving vehicle during its run through the swirling flow generated by the tornado simulator. The horizontal axis indicates the position of the vehicle centre. The each coefficient was calculated by using the maximum tangential velocity, *Vmax*. Due to the nature of the swirling flow, the shape of the side force should be symmetric with respect to the origin, and those of the lift force and yawing moment should be symmetric with respect to the vertical axis. As seen the figure, our results show this tendency to a certain degree. However, the side force becomes positive and the yawing moment become maximum before the vehicle reaches the vortex centre. The yawing moment does not decrease to negative values at $x/R > 0$ while it does at $x/R < 0$. The lift force has a second peak at $x/R = -2$, but it does not at $x/R = 2$. These suggest that the vehicle deforms the flow structure when it runs through the swirling flow.

4 Concluding remarks

The experimental method was developed to clarify the flow around the moving vehicle in the tornado. The tornado simulator and the moving model rig were developed to perform the experiment. The flow field generated by the tornado simulator was verified by comparing with the radar data of the full-scale tornado and the Rankin vortex model. The aerodynamic forces acting on the vehicle in the swirling flow were successfully obtained. The result suggests the vehicle affects the flow structure.

PIV measurements are planned to clarify the flow structure around the static/moving vehicle in the swirling flow.

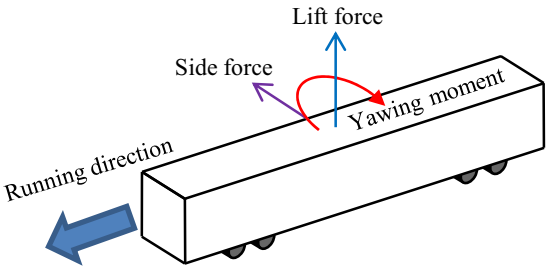

Figure 7. Definition of aerodynamic forces and yawing moment acting on the vehicle.

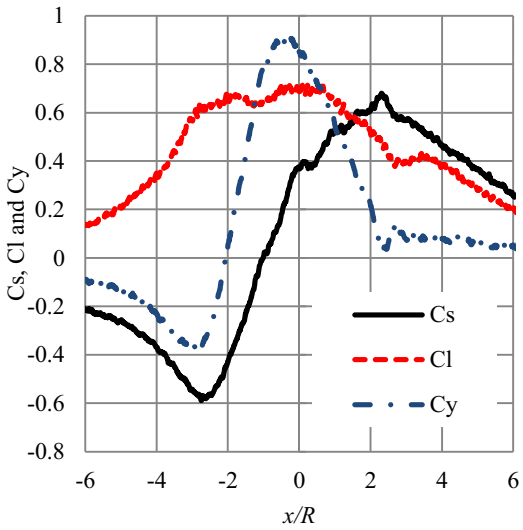

Figure 8. Ensemble averaged time histories of side and lift forces and yawing moment acting on the vehicle.

Acknowledgements

This work was supported by JSPS KAKEN Grant Number 26350491.

References

1. Aircraft and Railway Accidents Investigation Commission, Railway accident analysis report RA2008-4, (2008) (in Japanese)
2. Aircraft and Railway Accidents Investigation Commission, Railway accident analysis report RA2008-6, (2008) (in Japanese)
3. F. L. Hann, P. P. Sarkar and W. A. Gallus, Eng. Structures **30**, 1146-1159 (2008)
4. American Nuclear Society, An American national standard, ANSI/ANS-2.3-2011 (2011)